IMPROVING THE SENSITIVITY OF ASTRONOMICAL CURVATURE WAVEFRONT SENSOR USING DUAL-STROKE CURVATURE: A SYNOPSIS

MALA MATEEN

1. Abstract

Below I present a synopsis of the paper: Improving the Sensitivity of Astronomical Curvature Wavefront Sensor Using Dual-Stroke Curvature, [1]. The paper discusses the technique of curvature wavefront sensing and compares it to other traditional wavefront sensors. It explains the limitation of curvature wavefront sensing and proposes a method to improve its sensitivity. The paper goes on to explain the implementation of the improved curvature wavefront sensor (CWFS).

2. Introduction

All large ground based telescopes ($\geq 8\,m$) use adaptive optics (AO) to correct for atmospheric aberrations so that a clear observation can be made. However before this correction can be made the aberrated wavefront has to be sensed by a wavefront sensor (WFS) which records the phase and amplitude of the wave. The measured aberrated signal is compared to a standard signal and the difference of the two is used to drive a deformable mirror which moves so as to correct the wavefront aberrations. Using a WFS that offers high sensitivity is critical for, astronomical observations where the guide star is usually faint, leading to a photon-starved detector, and for extreme-AO where the large number of elements and short sampling time make the system photon-starved even on bright sources.

Shack-Hartmann WFSs (SHWFSs) are traditionally used on AO systems, they are able to close the loop even with large wavefront errors and perform well on extended targets. Curvature WFSs (CWFSs) are less commonly used but are very successful in measuring wavefronts from faint guide stars [2]. There are several benefits to using a CWFS over a SHWFS. Only one CWFS subaperture is needed per DM actuator as opposed to 4 or more SHWFS per DM actuator. The optical gain (which quantifies how phase aberrations are transformed into intensity signal by the WFS) can be tuned just by moving the vibrating membrane whereas on a SHWFS one would need to change the subaperture size. CWFSs are also able to obtain higher Strehl ratios compared to SHWFs.

CWFSs measure wavefront phase aberration by acquiring two intensity images on either side of the pupil plane. In high-order systems CWFSs lose sensitivity to low spatial frequency wavefront

---

Date: November 2, 2009.

aberrations. This effect referred to as ”noise-propagation” limits the usefulness of curvature wavefront sensing for high-order AO systems and/or large telescopes. The paper discusses how this noise propagation occurs and how this limitation can be overcome by acquiring four defocused images of the pupil instead of two.

3. Curvature Wavefront Sensing

In a CWFS, light intensity is measured in planes optically conjugated on either sides of the telescope pupil, [3]. These are referred to as the defocused pupil planes. A vibrating membrane placed at the focal plane is used to alternate between the two defocused planes. The distance from the pupil plane to the defocused plane is given by:

$$z = -\frac{f_1^2}{f_m}. \tag{1}$$

where f_1 is the focal length of the beam delivered to the VM and f_m is the VM's focal length. CWFSs rely on Fresnel propagation over the distance z to transform phase aberrations into intensity fluctuations. Consider a complex amplitude $W(\mathbf{u}, z)$, where $\mathbf{u}$ is the 2D coordinate on a plane perpendicular to the optical axis and z is the coordinate along the optical axis. A pupil plane optical path difference (OPD) aberration of spatial frequency $\mathbf{f}$, spatial phase θ, and amplitude h corresponding to the complex amplitude

$$W(\mathbf{u}, 0) = exp[i\frac{2\pi h}{\lambda} sin(2\pi \mathbf{uf} + \theta)]. \tag{2}$$

is transformed, after propagation over z, into

$$W(\mathbf{u}, 0) = exp[e^{id\phi} \times i\frac{2\pi h}{\lambda} sin(2\pi \mathbf{uf} + \theta)]. \tag{3}$$

where $d\phi = \pi|f|^2 z\lambda$, $e^{id\phi}$ is called the transfer function, and z is Fresnel propagation distance. If the propagation distance z is such that $d\phi = \pi/2$, $W(\mathbf{u}, z)$ is real: Fresnel propagation has transformed the phase aberration into a pure intensity aberration. If $d\phi$ is a multiple of 2π, the propagated OPD is a copy of the original OPD and is purely phase. This effect that replicates linear spatial frequencies at set intervals is known as the Talbot Effect and the distance z at which the magnitude of the amplitude repeats is known as the Talbot distance. The authors propose to set the defocused pupil planes at this distance. The contrast between the defocused images $W_+ = |W(\mathbf{u}, z_+)|^2$ and $W_- = |W(\mathbf{u}, z_-)|^2$ is

$$C = \frac{W_+ - W_-}{W_+ + W_-} = tanh[2\, sin(d\phi)\frac{2\pi h}{\lambda} sin(2\pi \mathbf{uf} + \theta)]. \tag{4}$$

The steps described above, which transform phase aberrations into intensity modulations, are illustrated in Figure 1, where the OPD aberration in the pupil is transformed via propagation into intensity variation on either side of the pupil plane. It can be seen that high spatial frequencies are most easily visible in planes conjugated close to the pupil plane, while low spatial frequencies are most obvious when looking further away from the pupil plane. For example consider an aberration with a period of $2\,m$, for low spatial frequency $d\phi = \pi/2$ at large z, far from the pupil. But for high spatial frequencies $d\phi = \pi/2$ at small z much closer to the pupil plane. For spatial frequencies which can be corrected by the AO system $d\phi < 1$ and $4\pi h sin(d\phi)/\lambda < 1$, and equation (4) becomes

$$C \approx 4\pi^2 f^2 z h sin(2\pi \mathbf{u}\mathbf{f} + \theta) \tag{5}$$

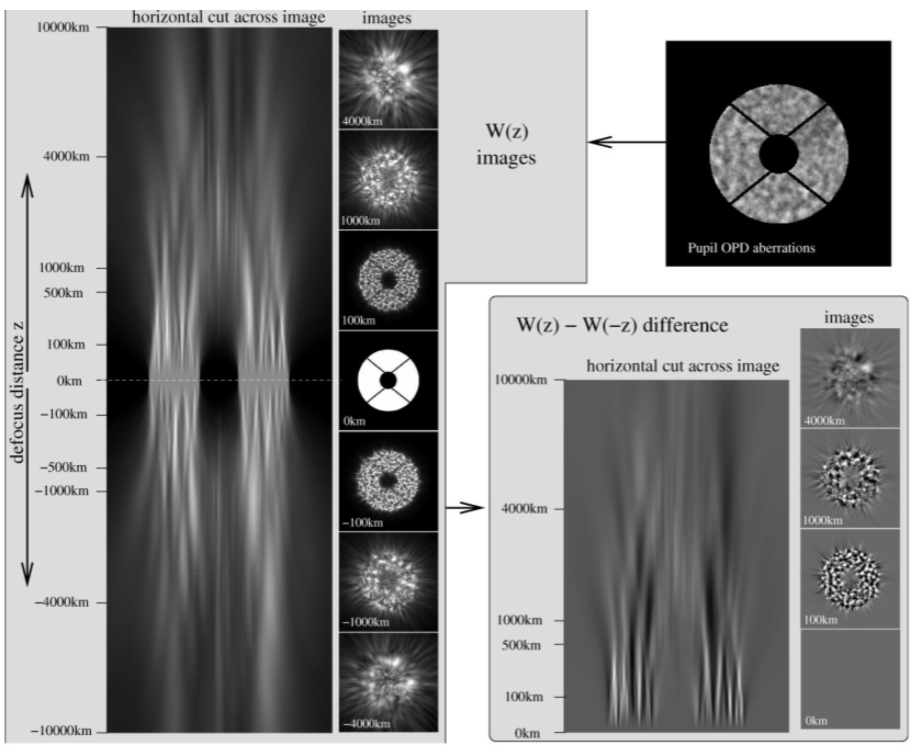

FIGURE 1. Simulations illustrating CWFS measurements. The pupil OPD measurements (upper right panel) are transformed into intensity fluctuations (left panel) by Fresnel propagation over a distance z. The difference in intensity obtained on either side of the pupil $W(z)$, $W(-z)$ gives the wavefront curvature (lower right panel).

4. Limitations of the Curvature Wavefront Sensor

In compliance with the curvature wavefront sensing theory it can be seen that C is proportional to the second derivative (curvature) of the wavefront's OPD. Equations (4) and (5) show that with larger z the conversion from phase to intensity is more efficient, z acts as an optical gain in the CWFS and therefore should be chosen large. There are however limits to how much z can be increased. Conventional curvature wavefront sensing relies on linearity of the WFS measurement. The contrast C measured should be proportional to the second derivative of the wavefront. For this to be true $sin(d\phi) \approx d\phi$ must be valid and $4\pi h sin(d\phi)/\lambda$ must be less than 1. If the constraint $d\phi \ll \pi$ is not satisfied then the WFS signal is no longer linear and equation (5) is no longer valid. If $d\phi > \pi$, $sin(d\phi)$ and $d\phi$ can have opposite signs, in which case the CWFS will produce a signal with a sign opposite to the actual wavefront. Equation (5) would then lead to runway amplification of high spatial frequencies. This constrains $d\phi$ to be less than π at high spatial frequencies. For $d\phi < \pi$ and with the Fresnel kernel substitution for spatial frequency ($f = x/\lambda z$) where z defines optical axis and x is the one dimensional aperture

$$z = \frac{4D^2}{N^2\lambda}. \tag{6}$$

here z is Fresnel propagation distance for the specific spatial frequency f, D is the pupil diameter, N is the number of wavefront sensor elements, and λ is the wavelength of observation. A qualitative model exploring the range of z distances shows that as the number of actuators increases, the defocus distance shrinks, and sensing of low-order aberrations becomes increasingly inefficient ($d\phi$ is much smaller than $\pi/2$). For low-order CWFS systems, the defocus distance decreases very rapidly with increasing number of actuators. In the mid-order domain the WFSs benefits from AO correction, and the speed at which the defocus distance drops is greatly slowed down; the benefit of having more actuators still outweighs the penalty of shorter defocus distances. When the actuator size becomes comparable to r_0, defocus distance drops more rapidly again, and the large number of actuators is only beneficial for very bright guide stars.

The ability of a CWFS to efficiently sense low-order aberrations decreases as the actuator density increases. Therefore as the guide star becomes fainter, the corrected wavefront degrades, which in turn reduces the defocus distance, and the sensitivity to sense low-order modes.

5. Linear Dual-Stroke Curvature Wavefront Sensing Principle

In the conventional CWFS increasing the number of actuators reduces sensitivity of low-order aberrations. Therefore a compromise needs to be made between two opposite requirements. A high number of actuators is necessary to achieve high Strehl ratios on bright guide stars, and a low number of actuators is needed to maintain sensitivity for faint guide stars. This means that the CWFS can either be tuned for high-order aberrations and bright targets (small defocus distance) or low-order aberrations and faint targets (large defocus distance) but can not efficiently measure both. This limitation is referred to as the noise-propagation effect. The paper presents a solution to this limitation. The solution, illustrated in Figure 2 is to incorporate two defocus distances dz_1 and dz_2, for small and large defocus distances respectively. The second sensor with a large defocus distance is dedicated to low-order aberrations. In this arrangement the light needs to be split 50/50 between the two WFSs, however the large gain in sensitivity in sensing low-order aberrations outweighs the loss of light for high-order aberrations. The gain in sensitivity for low-order aberrations is equivalent to increasing the stellar brightness by a factor of $0.5 \times (dz_2/dz_1)^2$, while the loss of light for high-order aberrations is equivalent to reducing the number of photons by half. In most cases the ratio dz_2/dz_1 is about 3. To implement the CWFS system with two defocus distances we need to figure out how to modify the hardware to achieve the two defocus distances.

6. Obtaining the Dual Defocus with a Vibrating Membrane Mirror

In conventional CWFS a vibrating reflective membrane is used to rapidly alternate between defocus distances. A speaker produces acoustic waves at a single frequency, chosen to excite the membrane's fundamental frequency. The membrane's vertical displacement excluding piston is given by function $Ar^2sin(2\pi ft)$, where r is the distance from the membrane center, f and A are the frequency and amplitude respectively, of the input electrical signal fed to the speaker. The idea is to modify this WFS scheme to accommodate two wavefront sensing modes. Instead of building a WFS per defocus altitude and using a beam splitter to divert light to the two WFSs the authors propose driving the defocusing vibrating membrane (VM) at two different frequencies to produce four defocused pupil planes, $+dz_1$, $-dz_1$, $+dz_2$, $-dz_2$, which are imaged onto the same detector.

In dual-stroke CWFS, a single period of low-amplitude (dz_1) sine wave immediately followed by a single period of higher amplitude (dz_2) sine wave is applied to the VM. If greater than 50% of photons are to be allocated to one of the WFSs than the sine waves for the two WFSs can have different periods. This whole pattern is repeated at $\approx KHz$ frequency. The VM can be made to produce different waveforms by using an iterative algorithm. A laser beam is shone on the center of the VM and a position sensing device (PSD) is used to measure the position of the VM in real-time. The laser beam is then shown off-center to measure the membrane curvature. The difference between the the input electrical signal E(t) and the output membrane M(t) is sufficient to recover the frequency response (both amplitude and phase) of the speaker-acoustic cavity assembly. This frequency response is used to update E(t) such that M(t) matches the desired membrane motion.

7. Results and Conlusion

Simulations implementing the 8 m Subaru Telescope pupil with 188 element curvature AO system were performed by the authors to quantify the gain in performance of the the single-stroke and dual-stroke curvature systems. A direct comparison between the gain of the two modes is shown

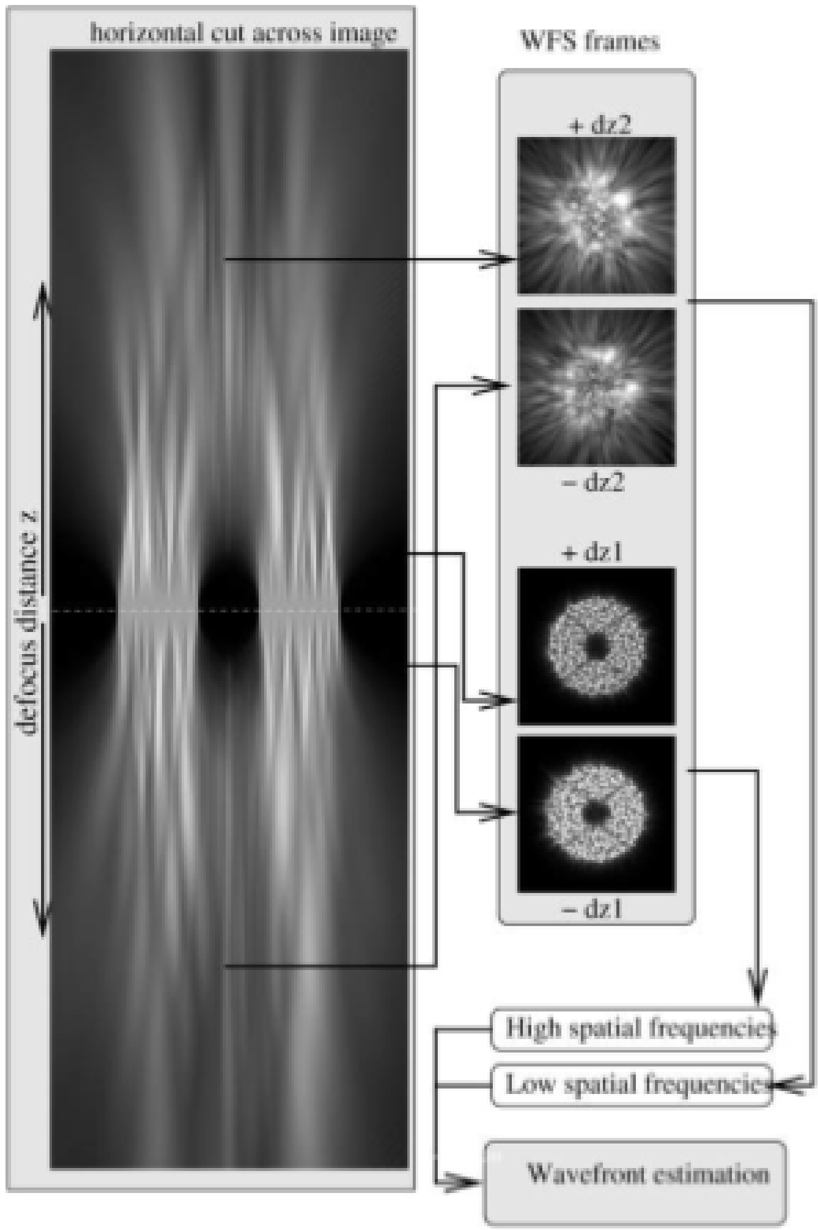

FIGURE 2. Principle of dual-stroke curvature wavefronts sensing. Four defocused pupil plane images are acquired by the WFS. Two short defocused distances ($\pm\, dz_1$) are used to extract high spatial frequencies and two long defocused distances ($\pm\, dz_2$) are used to extract low spatial frequencies.

in Figure 3. They find that performance is optimal when $dz_2 = 3 \times dz_1$ and dz_1 is very close to optimal defocus distance determined, using equation (6), for a single-stroke system. In comparison of Strehl ratio a full stellar magnitude is gained in sensitivity by adopting the dual-stroke scheme. The largest gain is obtained for low-order aberrations (especially tip/tilt) that benefit from a longer defocus distance. A comparison of the PSF between single and dual stroke systems for low order modes shows that the dual stroke PSF is crisper and displays higher contrast.

The paper concludes that dual-stroke wavefront sensing technique offers significant performance gain over conventional single-stroke curvature wavefront sensors. It has also been shown that implementing a dual-stroke scheme requires the same apparatus as the single-stroke scheme; the only difference being that the existing VM is driven to four defocused pupil planes instead of two.

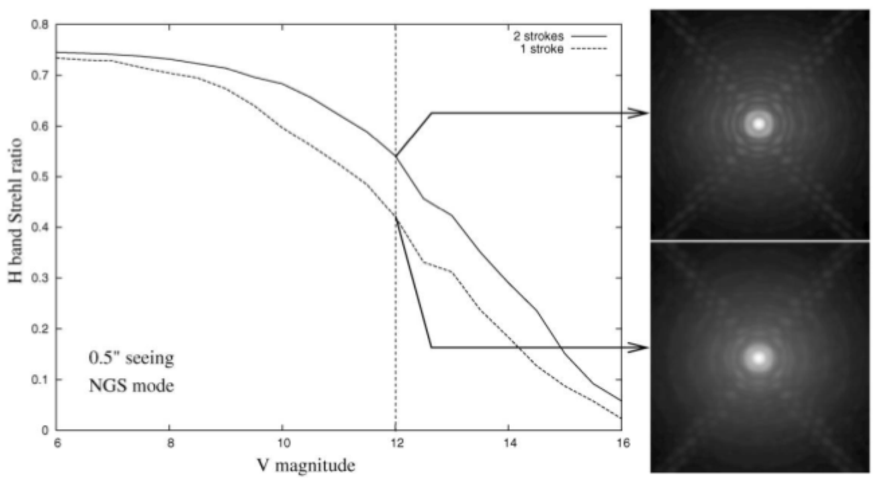

FIGURE 3. A comparison of simulated H band Strehl ratio as a function of guide star magnitude for single and dual stroke schemes. With the dual stroke mode a sensitivity gain of 1 to 1.5 stellar magnitude is obtained. Single and dual stroke PSFs obtained for a 12 magnitude star are shown on the right.

References

[1] O. Guyon, C. Blain, H. Takami, Y. Hayano, M. Hattori, and M. Watanabe. Improving the Sensitivity of Astronomical Curvature Wavefront Sensor Using Dual-Stroke Curvature. *PASP*, 120:655–664, May 2008.

[2] F. Roddier. Curvature sensing and compensation: a new concept in adaptive optics. *Applied Optics*, 27:1223–1225, April 1988.

[3] F. Roddier, M. Northcott, and J. E. Graves. A simple low-order adaptive optics system for near-infrared applications. *PASP*, 103:131–149, January 1991.

1630 East University Blvd. Tucson AZ 85721 College of Optical Sciences, University of Arizona